Regular Article

blood

THROMBOSIS AND HEMOSTASIS

Polyphosphate nanoparticles on the platelet surface trigger contact system activation

Johan J. F. Verhoef,[1,*] Arjan D. Barendrecht,[2,*] Katrin F. Nickel,[3,4,*] Kim Dijkxhoorn,[2] Ellinor Kenne,[3] Linda Labberton,[3] Owen J. T. McCarty,[5] Raymond Schiffelers,[2] Harry F. Heijnen,[2] Antoni P. Hendrickx,[6] Huub Schellekens,[1] Marcel H. Fens,[2] Steven de Maat,[2] Thomas Renné,[3,4] and Coen Maas[2]

[1]Department of Pharmaceutics, Utrecht Institute for Pharmaceutical Sciences, Utrecht University, Utrecht, The Netherlands; [2]Department of Clinical Chemistry and Haematology, University Medical Center Utrecht, Utrecht, The Netherlands; [3]Department of Molecular Medicine and Surgery, Karolinska Institutet and University Hospital, Stockholm, Sweden; [4]Institute of Clinical Chemistry and Laboratory Medicine, University Medical Center Hamburg-Eppendorf, Hamburg, Germany; [5]Department of Biomedical Engineering, Department of Cell & Developmental Biology, Division of Hematology & Medical Oncology, Oregon Health & Science University, Portland, OR; and [6]Department of Medical Microbiology, University Medical Center Utrecht, Utrecht, The Netherlands

Key Points

- Activated platelets expose insoluble membrane-associated polyphosphate nanoparticles that are complexed with divalent metal ions.
- Platelet polyphosphate nanoparticles, but not soluble polyphosphate polymers, activate the contact system.

Polyphosphate is an inorganic polymer that can potentiate several interactions in the blood coagulation system. Blood platelets contain polyphosphate, and the secretion of platelet-derived polyphosphate has been associated with increased thrombus formation and activation of coagulation factor XII. However, the small polymer size of secreted platelet polyphosphate limits its capacity to activate factor XII in vitro. Thus, the mechanism by which platelet polyphosphate contributes to thrombus formation remains unclear. Using live-cell imaging, confocal and electron microscopy, we show that activated platelets retain polyphosphate on their cell surface. The apparent polymer size of membrane-associated polyphosphate largely exceeds that of secreted polyphosphate. Ultracentrifugation fractionation experiments revealed that membrane-associated platelet polyphosphate is condensed into insoluble spherical nanoparticles with divalent metal ions. In contrast to soluble polyphosphate, membrane-associated polyphosphate nanoparticles potently activate factor XII. Our findings identify membrane-associated polyphosphate in a nanoparticle state on the surface of activated platelets. We propose that these polyphosphate nanoparticles mechanistically link the procoagulant activity of platelets with the activation of coagulation factor XII. (*Blood*. 2017;129(12):1707-1717)

Introduction

Following the discovery of polyphosphate in mammalian cells, this inorganic, negatively charged polymer has been shown to be present in a variety of cell types, such as platelets,[1] mast cells,[2] and tumor cells.[3] Polyphosphate plays a role in a variety of hemostatic and thrombotic mechanisms. It enhances the binding of platelets to von Willebrand factor[4] (VWF), induces clustering of platelet factor 4 into antigenic complexes,[5] acts as a cofactor for C1 esterase inhibitor (C1inh),[6] triggers activation of factor XII (FXII),[7] amplifies factor XI (FXI) activation by thrombin,[8] accelerates factor V activation,[9] inactivates tissue factor pathway inhibitor,[10] inhibits fibrinolysis, and alters fibrin clot structure.[11] As a result, polyphosphate has been proposed as a potential druggable target to prevent thrombosis.[12-14]

In preclinical in vivo studies using experimental models of thrombosis, selective depletion of (or deficiency in) coagulation FXII was consistently found to confer protection against thrombosis without increasing bleeding.[15-18] Collective evidence from decades of research had previously established that platelet activation is associated with activation of FXII.[19-22] More recent studies implicate platelet polyphosphate as an endogenous trigger for FXII activation in thrombus formation in vivo.[23] However, when platelets become activated, only short polyphosphate polymers (60-100 residues) are secreted into the surrounding fluid. These short-chain soluble polyphosphates have a surprisingly low capacity for direct activation of FXII in vitro.[24-26] This observation suggests that we are lacking essential insight into the mechanistic link between platelet polyphosphates and FXII during thrombus formation in vivo.

In addition to polyphosphate (130 mM),[1] intracellular granules contain large amounts of inorganic compounds, such as adenosine triphosphate (400 mM), adenosine diphosphate (600 mM), pyrophosphate (300 mM), and serotonin (65 mM),[27] and are characterized by a low pH of ~5.4.[28] Moreover, these organelles are rich in calcium (2.2 M) and other divalent metal ions. The steps involved in secretion of the content-dense granules are not fully defined. For polyphosphate, it is thought to be molecularly dissolved

Submitted 19 August 2016; accepted 23 December 2016. Prepublished online as *Blood* First Edition paper, 3 January 2017; DOI 10.1182/blood-2016-08-734988.

*J.J.F.V., A.D.B., and K.F.N. contributed equally to this study.

The online version of this article contains a data supplement.

There is an Inside *Blood* Commentary on this article in this issue.

The publication costs of this article were defrayed in part by page charge payment. Therefore, and solely to indicate this fact, this article is hereby marked "advertisement" in accordance with 18 USC section 1734.

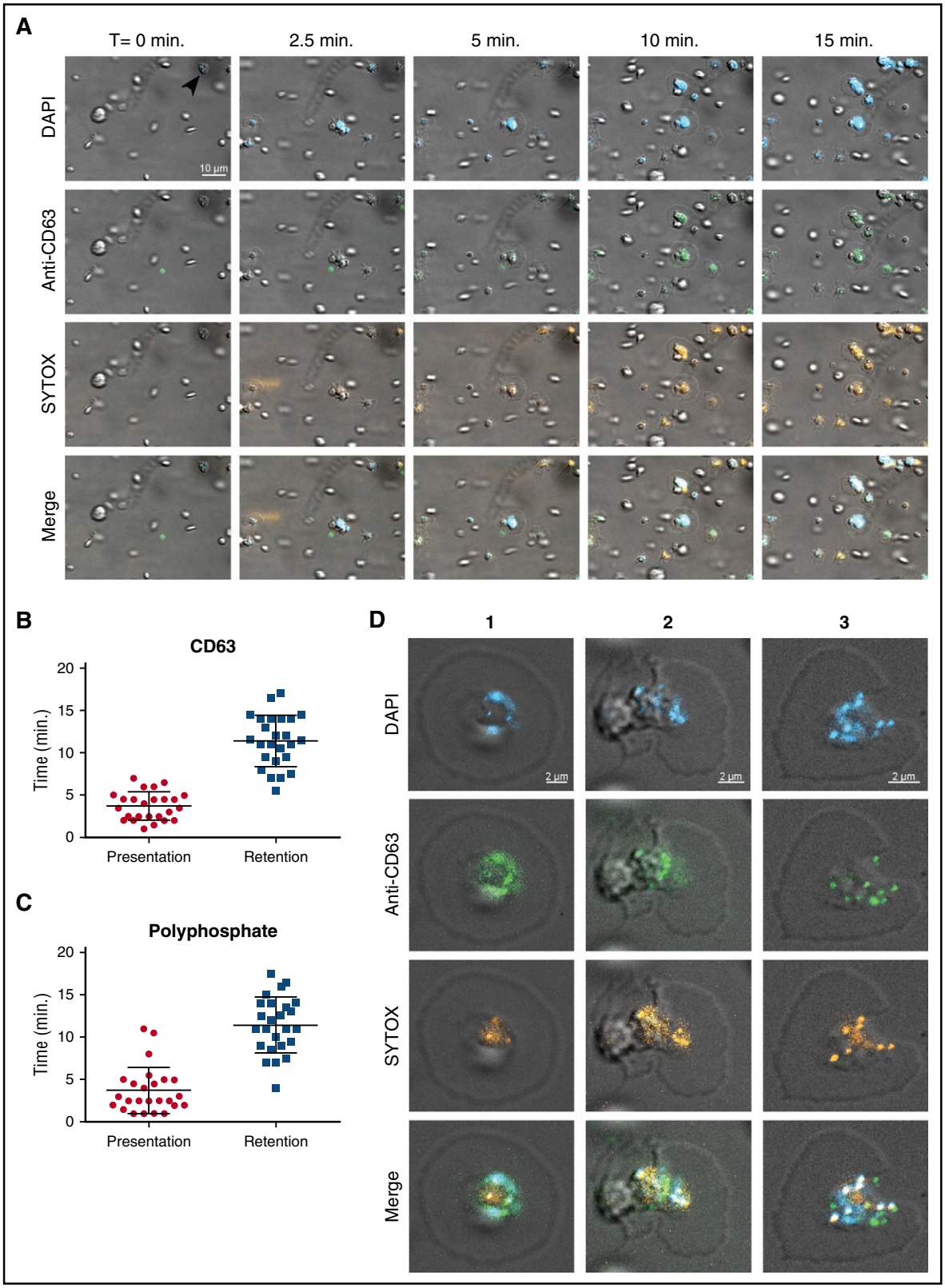

Figure 1. Polyphosphate is retained on the platelet surface after degranulation. (A) Time series of platelet adhesion and spreading on immobilized VWF under flow. Polyphosphate was tracked with DAPI (blue) and SYTOX (orange). Degranulation was detected by an anti-CD63 antibody (green). Microscopic images were acquired at a magnification of ×1000. A scale bar is shown in the upper left panel (10 μm). All images are shown at the same magnification. Times (above) represent the time course, starting from the moment of first stable platelet adhesion in the image field (indicated by arrow in upper left panel). (B-C) Individual spreading platelets were visually inspected ($n = 25$, derived from videos of >3 separate experiments). Approximately 4 minutes after initial adhesion, both CD63 and polyphosphate appeared on the platelet surface ("Presentation"'). The fluorescence of both these markers persisted for the remainder of the experiments ("Retention"). (D) Localization of polyphosphate and CD63 on spreading platelets after >20 minutes. T, time.

Table 1. Colocalization between DAPI, SYTOX, and CD63 on the platelet surface

Anti-CD63 with SYTOX, %	DAPI with SYTOX, %	DAPI with anti-CD63, %
40 ± 8	50 ± 13	48 ± 12

Colocalization of anti-CD63, DAPI, and SYTOX staining was determined by means of pixel intensity correlation on confocal images.

and directly released into the extracellular environment after platelet activation.[29]

We report here that, in addition to soluble secreted polyphosphate, a previously unidentified second pool of polyphosphate exists in platelets. This species of polyphosphate forms nanoparticles, composed of polyphosphate and divalent metal ions, and remains associated with the platelet surface after degranulation. Platelet polyphosphate nanoparticles constitute a powerful activator of FXII, providing the "missing link" between primary hemostasis and activation of the contact pathway of coagulation.

Materials and methods

A detailed description of "Materials and methods" with additional information is provided in the supplemental Data, available on the *Blood* Web site.

Platelet isolation

Platelets were isolated from citrated blood of healthy volunteers under approval of the local Medical Ethical Committee of the University Medical Center Utrecht by centrifugation.

Production of recombinant exopolyphosphatase and a truncated variant

Exopolyphosphatase (PPX) or its polyphosphate-binding domains (PPX_Δ12) were expressed in *Escherichia coli* and purified as previously published with minor modifications.[14] After purification, the PPX and the PPX_Δ12 were dialyzed against phosphate buffer (10 mM Na_2HPO_4, 10 mM NaH_2PO_4, 500 mM NaCl, pH 7.4).

Live-cell imaging under flow

Washed platelet suspensions were supplemented with Alexa488-labeled anti-CD63 to visualize dense granule degranulation and 1.5 μM SYTOX Orange (Molecular Probes/Life Technologies, Waltham, MA) or 5 μg/mL Alexa488-conjugated PPX_Δ12 to visualize polyphosphate, and subsequently perfused through a laminar-flow chamber[30] over VWF-coated cover glasses at low shear rates (25-50 s^{-1}). In selected experiments, platelets were preincubated for 30 minutes at 37°C with 10 μg/mL 4′,6-diamidino-2-phenylindole (DAPI; Sigma-Aldrich Chemie, Zwijndrecht, The Netherlands) and centrifuged at 400*g* for 15 minutes in the presence of 10 ng/mL prostacyclin to remove unbound dye. Where indicated, the effect of ethylenediaminetetraacetic acid (EDTA; 50-500 mM), 10 μg/mL ribonuclease A (Invitrogen, Bleiswijk, The Netherlands), 10 μg/mL deoxyribonuclease I (Roche, Mannheim, Germany), or 500 μg/mL PPX was investigated. In plasma experiments, platelet adhesion, spreading, and degranulation were studied step-wise in the continuous presence of SYTOX Orange. First, platelet-rich plasma was perfused over immobilized fibrinogen at a shear rate of 25 s^{-1} for 10 minutes. Next, unbound platelets were removed by perfusion with platelet-poor plasma for 5 minutes. Finally, adherent platelets were activated by perfusion with PAR4-activating peptide (Bachem, Bubendorf, Switzerland) in platelet-poor plasma for another 10 minutes. Polyphosphate deposition during thrombus formation was investigated by perfusing citrated whole blood over collagen-coated cover glasses at a high shear rate (1600 s^{-1}). Analyses were performed on a Zeiss Z1 microscope with Colibri LEDs and ZEN 2 Blue Edition software. Videos were captured at a magnification of ×1000 for 20 to 40 minutes at a frame rate of 2 frames per minute. After perfusion experiments, cover glasses were removed from the flow chambers and studied further by confocal microscopy and scanning electron microscopy. A detailed description is provided in the supplemental Data.

Platelet fractionation by density ultracentrifugation

Washed platelets (2.5×10^6/mL) were resuspended in lysis buffer (25 mM HEPES [*N*-2-hydroxyethylpiperazine-*N*′-2-ethanesulfonic acid], 250 mM sucrose, 12 mM sodium citrate, pH 6.5) with 1 mM sodium orthovanadate and 1:100 protease inhibitor cocktail (p8340; Sigma-Aldrich) and lysed by 3 pulses of mild sonication (5 seconds at 3 mV) on a Soniprep 150 (MSE, London, UK). Suspensions were subsequently centrifuged at 1000*g* for 15 minutes at 4°C; supernatants containing polyphosphate nanoparticles were collected on ice. The pelleted material was resuspended, sonicated, and centrifuged in 2 to 4 additional cycles until no more pellet was observed. Finally, the collected supernatants were combined and centrifuged at 19 000*g* for 20 minutes at 4°C. The pellet containing polyphosphate nanoparticles was diluted in 1.4 mL lysis buffer with 250 mM sucrose and supplemented with 5 μM SYTOX Orange. Where indicated, 250 mM EDTA was added. Samples were loaded on top of a sucrose gradient with 0.7 mL fractions ranging from 0.5 M to 2 M, diluted in lysis buffer without protease inhibitors. The gradient was centrifuged at 1 000 000*g* for 60 minutes at 4°C using a Beckman SW40 rotor (without brake). Fractions of 350 μL were analyzed for SYTOX Orange fluorescence at 540/570 nm excitation/emission using a Spectramax 340 (Molecular Devices, Sunnyvale, CA) plate reader. The phosphate content in SYTOX Orange–rich fractions was determined by means of acid digestion and subsequent reaction with ammonium molybdate as described by Rouser et al.[31]

Platelet polyphosphate extraction

Human pheresis platelets (~$2\text{-}4 \times 10^{11}$ platelets/pheresis unit) were obtained from the blood banks of Karolinska University Hospital and University Medical Center Hamburg and used for polyphosphate isolation within the expiry date (application in human transfusion). Polyphosphate was isolated by 2 different methods: (1) Isolation of soluble polyphosphate from lysed platelets by phenol/chloroform extraction was performed as previously described with minor modifications, described in the supplemental Data.[23] (2) Isolation of total polyphosphate from lysed platelets, including membrane-associated polyphosphate. A spin column anion exchanger method was performed as described[3] with some modifications, described in the supplemental Data. Polyphosphate concentrations were measured after hydrolysis in 1 M HCl at 95°C for 60 minutes. The orthophosphate released by polyphosphate digestion was estimated using colorimetric phosphate assay kit (Abcam) according to the manufacturer's instructions, and absorbance was measured at 650 nm with a Multiskan GO Microplate Spectrophotometer (Thermo Scientific).

Polyphosphate electrophoresis

Polyphosphate (1 nmol/lane of platelet-purified polyphosphate; expressed as monophosphate units, or 100 ng/lane of synthetic polyphosphate; indicated in figure legends) was separated by electrophoresis on 10% polyacrylamide tris-borate-EDTA buffer (TBE)-urea (7 M) gels and stained by DAPI-negative staining as previously described.[14] Alternatively, calcium-preadsorbed synthetic polyphosphate (70-mers; 40 μg/lane) was separated on 15% Urea-TBE gels[32] and stained with toluidine blue.[33] In some experiments, platelet polyphosphate extracts were incubated with alkaline phosphatase (PSP, 10 U/mL) in the presence of 5 mM $MgCl_2$ for 120 minutes at 37°C prior to separation. In other experiments, calcium-preadsorbed synthetic short polyphosphate (4 mg/mL) and PPX (concentration series) were dissolved in HT buffer containing 5 mM $MgCl_2$ and incubated at 37°C for 1 hour.

Plasma contact system activation with platelet polyphosphate

Venous blood was collected from healthy human volunteers into 3.2% trisodium citrate (9:1 blood-to-citrate ratio). The first 10 mL was discarded. Platelet-free plasma was prepared by 2 consecutive centrifugation steps at 3000*g* for 10 minutes. Plasma from individuals with congenital deficiency in FXII was purchased from George King Biomedical (Overland Park, KS). Either 1.5 μg/mL kaolin or 20 μM platelet-derived polyphosphate (expressed as monophosphate units) was used as a trigger. Optionally, 50 mM EDTA was added. Development of kallikrein-like activity was analyzed with 1 mM substrate

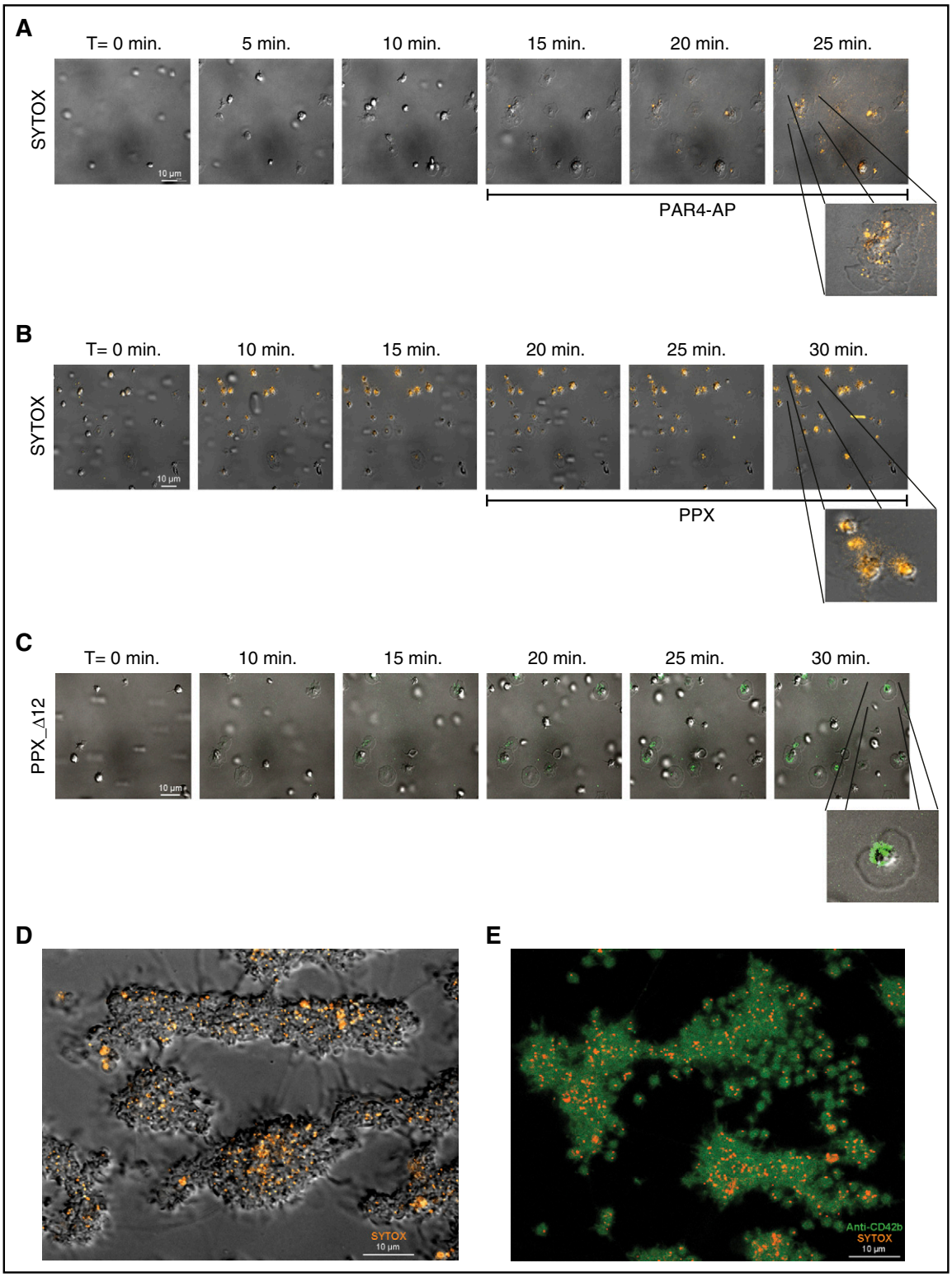

Figure 2. Membrane-associated polyphosphate is incorporated into platelet aggregates. Microscopic images were acquired at a magnification of ×1000 (A-D) and ×630 (E). Scale bar is shown in the left panels (10 μm). All images are shown at the same magnification; insets show indicated areas at higher magnification. Times (above) represent the time course, starting from the moment of first stable platelet adhesion in the image field. (A) Time series of spreading and degranulation of platelets in citrated plasma on immobilized fibrinogen at 25 s^{-1} shear rate during activation by PAR4-activating peptide (PAR4-AP). Polyphosphate was visualized with SYTOX (orange); PAR4-AP enters the flow chamber after 15 minutes of perfusion (indicated below the images). (B) Time series of platelet adhesion and spreading on immobilized VWF under flow. Polyphosphate was visualized with SYTOX (orange); PPX (500 μg/mL) enters the flow chamber after 20 minutes of perfusion (indicated below the images). (C) Time series of platelet adhesion and spreading on immobilized VWF under flow. Polyphosphate was visualized with Alexa488-conjugated PPX_Δ12 (green). (D-E) Cross-section images of SYTOX-stained platelet aggregates, formed by perfusing citrated whole blood over immobilized collagen at 1600 s^{-1} shear rate for 10 minutes. (D, bright-field/fluorescence microscopy image of unfixed aggregates; E, confocal microscopy image of fixed aggregates) Green, anti-CD42b; orange, SYTOX. Images are representative of experiments that were performed >3 times.

S-2302 (sensitive to FXIIa and plasma kallikrein; Chromogenix, Mölndal, Sweden) at an absorbance wavelength of 405 nm in a Bio-Kinetics Reader (BioTek Instruments Inc) at 37°C.

Plasma activation with short polyphosphate (70-mers) and enzyme-C1inh complex ELISAs

Prewarmed citrated plasma was activated by addition of 50 μg/mL calcium-preadsorbed polyphosphate.[23] Where indicated, 100 U/mL aprotinin was added prior to plasma activation. Where indicated, polyphosphate was incubated with EDTA, after which it was diluted to a final concentration of 50 μg/mL and 100 mM, respectively. Total kallikrein-like activity was monitored at 37°C by cleavage of the chromogenic substrate H-D-Pro-Phe-Arg-pNA (0.5 mM final concentration) at 405 nm. Alternatively, samples were collected in assay-specific buffer for analysis by enzyme-linked immunosorbent assay (ELISA). The C1inh-enzyme complex ELISA was performed as previously described.[34]

Results

Polyphosphate mobilization to the platelet surface

It was previously reported that platelet polyphosphate can be visualized with the cell-permeable dye DAPI.[1] We perfused DAPI-treated washed human platelets over immobilized VWF at a venous shear rate (25 s^{-1}). Under these conditions, DAPI-positive platelets adhere without aggregating. The fluorescent DAPI staining of platelets was consistent with localization of polyphosphate in dense granules[1] and persisted over the complete course of our experiments (Figure 1A blue). However, CD63 exposure on the surface indicated that platelet degranulation was spontaneously taking place under these conditions[35] (Figure 1A green; quantification in Figure 1B). Unlike DAPI, SYTOX is a cell-membrane impermeable nucleic acid stain that is commonly used to distinguish extracellular from intracellular DNA.[36] During degranulation, platelets began to display SYTOX fluorescence (Figure 1A orange; supplemental Video 1A-B; without and with DAPI, respectively). SYTOX fluorescence was detected on the platelet surface for prolonged periods of time, suggesting that polyphosphate is exposed and retained on the cell surface under flow (Figure 1C). In the majority of experiments, SYTOX-positive structures with spherical morphology were observed on the platelet surface. SYTOX fluorescence on the platelet surface was unaffected by deoxyribonuclease I or ribonuclease A (supplemental Figure 1A-B), indicating that the contribution of nucleic acids to this cell surface staining was negligible. We confirmed the activity of these enzymes in control experiments (supplemental Figure 1C-D). Analyses of platelet cell surfaces after 20 minutes of perfusion showed partial colocalization between DAPI, SYTOX, and anti-CD63 (Figure 1D; Table 1). Furthermore, SYTOX fluorescence on the surface of activated platelets persisted in the presence of plasma, indicating resistance against plasma phosphatase activity (Figure 2A; supplemental Video 2A). SYTOX fluorescence also persisted in the presence of recombinant PPX (Figure 2B; supplemental Video 2B) during the course of our experiments. We confirmed the enzymatic activity of PPX in control experiments (supplemental Figure 1E). However, we found that the distribution of polyphosphate on the platelet surface slowly became less punctate, suggesting some degradation by PPX. Furthermore, we observed that an antithrombotic variant of PPX, lacking its protease domain (PPX_Δ12),[14] bound to the surface of activated platelets (Figure 2C; supplemental Video 2C). The binding of this polyphosphate-specific probe further confirms that polyphosphate is retained on the membrane surface.

Finally, platelet aggregate formation in whole blood on immobilized collagen under high shear rates (1600 s^{-1}) revealed that polyphosphate was incorporated into the aggregates (Figure 2D-E). Supplemental Video 3A shows a sequence of microscopic images at varying distances from the surface (indicated above) of a SYTOX-stained platelet aggregate. Supplemental Video 3B shows a 3-dimensional reconstruction of SYTOX-stained platelet aggregates, analyzed by confocal microscopy.

These results suggest that platelets not only secrete soluble polyphosphate polymers into the surrounding solution, as was demonstrated earlier,[1,23] but also retain polyphosphate on their surface after degranulation. We subsequently went on to investigate the biochemical properties of platelet membrane-associated polyphosphate.

Platelet polyphosphate exists in 2 pools and displays nanoparticle-like behavior

Previous studies that identified platelet polyphosphate with a short polymer size in supernatant from platelets employed a phenol/chloroform extraction method for purification.[23] This extraction method is selective for soluble secreted molecules due to the removal of all cellular and cell-bound materials. Confirming our previous reports,[3,23] we found polyphosphate polymers with an apparent size of 60 to 90 units in platelet lysates when extracted by phenol/chloroform extraction (Figure 3A). We subsequently extracted polyphosphate from complete platelet lysate by anion-exchange purification, which should purify all polyphosphate independently of polymer size, subcellular localization, or solubility. In this preparation, polyphosphate polymers displayed a larger apparent size and chain length distribution. Digestion of the extracted material with phosphatase (PSP) completely ablated the signal (Figure 3A). Moreover, polyphosphate with large apparent polymers sizes were found in multiple individual donors when isolated from complete platelet lysate by anion-exchange purification (Figure 3B).

We next investigated the contact system–activating properties of polyphosphate extracted by these 2 methods. Total platelet polyphosphate (Ion exc; 20 μM, expressed as monophosphate units) strongly activated the plasma contact system, as determined in a chromogenic assay for kallikrein-like activity in plasma, while soluble polymers (phenol/chloroform; 20 μM, expressed as monophosphate units) were poor activators (Figure 3C). Plasma contact system activation was critically dependent on the presence of FXII (Figure 3C; ΔFXII indicates congenital FXII-deficient plasma). These findings indicate that, in addition to soluble short-chain polyphosphate polymers,[1] a second polyphosphate pool with a higher apparent polymer size is present in platelets, which remains associated with the cell surface after secretion. To further investigate this concept, we lysed platelets in the presence of SYTOX. We then fractionated these lysates by sucrose density ultracentrifugation. SYTOX fluorescence was particularly enriched in a subset of fractions with higher sucrose densities (Figure 3D, group II). These, as well as surrounding control fractions (Figure 3D, group I and III), were collected for further analysis. In control experiments, we confirmed that SYTOX without platelet lysate (ie, unbound free dye) does not display any fluorescence or sedimentation behavior (not shown). Determination of the average hydrodynamic diameter of particles in the collected fractions revealed that SYTOX fluorescence was mainly associated with a population of particles that had an average hydrodynamic size of 554 nm (Table 2). Pooled samples from SYTOX-rich fractions 21 to 25 (100-μL samples from each fraction; 500 μL total volume) typically contained 820.1 μg phosphate. When we analyzed these fractions further by microscopy,

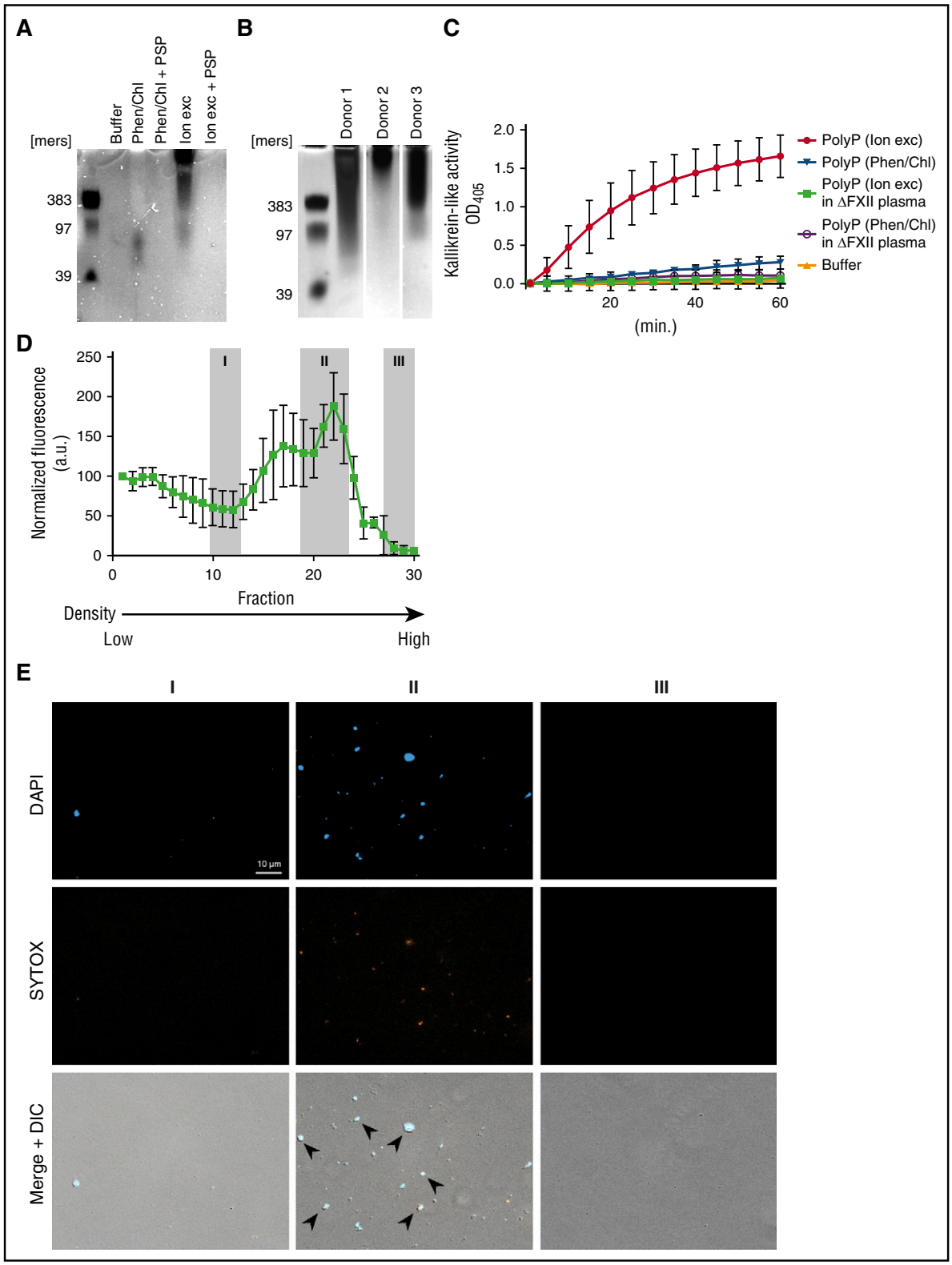

Figure 3. Platelet polyphosphate exists in 2 pools and displays nanoparticle-like behavior. (A) Gel electrophoresis of soluble platelet polyphosphate (phenol/chloroform [Phen/Chl]) or total platelet polyphosphate (ion exchange [Ion exe]). Polyphosphate (1 nmol/lane; expressed as monophosphate units) was separated on 10% polyacrylamide TBE-urea (7 M) gels and visualized by DAPI-negative staining. PSP (10 U/mL) indicates phosphatase treatment prior to separation. Synthetic polyphosphate preparations with polymer sizes of 39, 97, and 383 phosphate units served as molecular size standard. A representative image for 3 separate experiments is shown. (B) Total platelet polyphosphate (Ion exc; 1 nmol/lane, expressed as monophosphate units) from 3 individual donors. (C) Kallikrein-like activity, triggered by platelet polyphosphate (PolyP), from 2 different sources (20 μM; expressed as monophosphate units). ΔFXII plasma indicates congenital FXII-deficient plasma. (D) Fractionation of SYTOX-supplemented platelet lysate by ultracentrifugation on sucrose density gradients. Data show normalized means ± standard deviation of 3 independent fractionation studies. (E) Microscopic images (acquired at ×1000 magnification) of representative samples that were taken from fractions, indicated in panel D by roman numerals I-III. Polyphosphate was detected with DAPI (blue) and SYTOX (orange). DIC, differential interference contrast microscopy; OD_{405}, optical density at 405 nm.

particles were found with affinity for both DAPI and SYTOX (Figure 3E roman numerals above the images refer to the fractions in Figure 3D).

Polyphosphate nanoparticles are retained at the platelet granulomere after release

Both our live-cell flow and fractionation studies indicated that platelet polyphosphate takes on a particulate state and accumulates on the surface of procoagulant platelets. We next analyzed the morphology and subcellular localization of platelet membrane-bound polyphosphate by confocal microscopy. Polyphosphate nanoparticles were positioned on top of the platelet granulomere of spread platelets (Figure 4A,B; supplemental Video 4; total polyphosphate in blue; extracellular polyphosphate in orange). Consistently, scanning electron microscopy revealed that spherical particles were present on the granulomere of spread platelets (Figure 4C). These particles range between 100 and 200 nm in diameter, which is comparable to particles formed by synthetic polyphosphate in the presence of calcium ions.[29]

Polyphosphate nanoparticle formation depends on divalent metal ion incorporation

Polyphosphate precipitates with divalent metal ions that are known to be highly abundant in dense granules.[28] Furthermore, it has been reported that synthetic polyphosphate forms insoluble stable nanoparticles in the presence of calcium ions.[29] We therefore investigated the effect of EDTA (a chelator of divalent metal ions) on platelet polyphosphate complexes. The presence of EDTA strongly reduced migration of SYTOX into the deeper, sucrose-dense fractions during ultracentrifugation fractionation of platelet lysates (Figure 5A). The phosphate content in fractions 21 to 25 was typically reduced by ~50% (457.2 μg) in the presence of EDTA, compared with the control situation (820.1 μg). In the presence of EDTA, SYTOX fluorescence remained concentrated in fractions with low sucrose densities, which we assume to contain soluble polyphosphate. These experiments indicate that SYTOX fluorescence is associated with polyphosphate-metal ion complexes.

We next investigated the properties of membrane-associated polyphosphate. Scanning electron microscopy revealed that spherical nanoparticles were no longer present on the platelet surface after exposure to EDTA (Figure 5B), underlining the role of divalent metal ions for polyphosphate nanoparticle formation. We next perfused

Table 2. Dynamic light scattering analyses of density fractions from platelet lysate

Fraction	I	II	III
Z-average (nm)	345	554	714
Polydispersity index	0.162	0.211	0.314

Mean hydrodynamic size (Z-average) in nanometers and polydispersity (0-1) of particles in subset of pooled fractions obtained after sucrose gradient ultracentrifugation of lysed platelets. Pooled fractions were derived from different density categories, as indicated in Figure 3D.

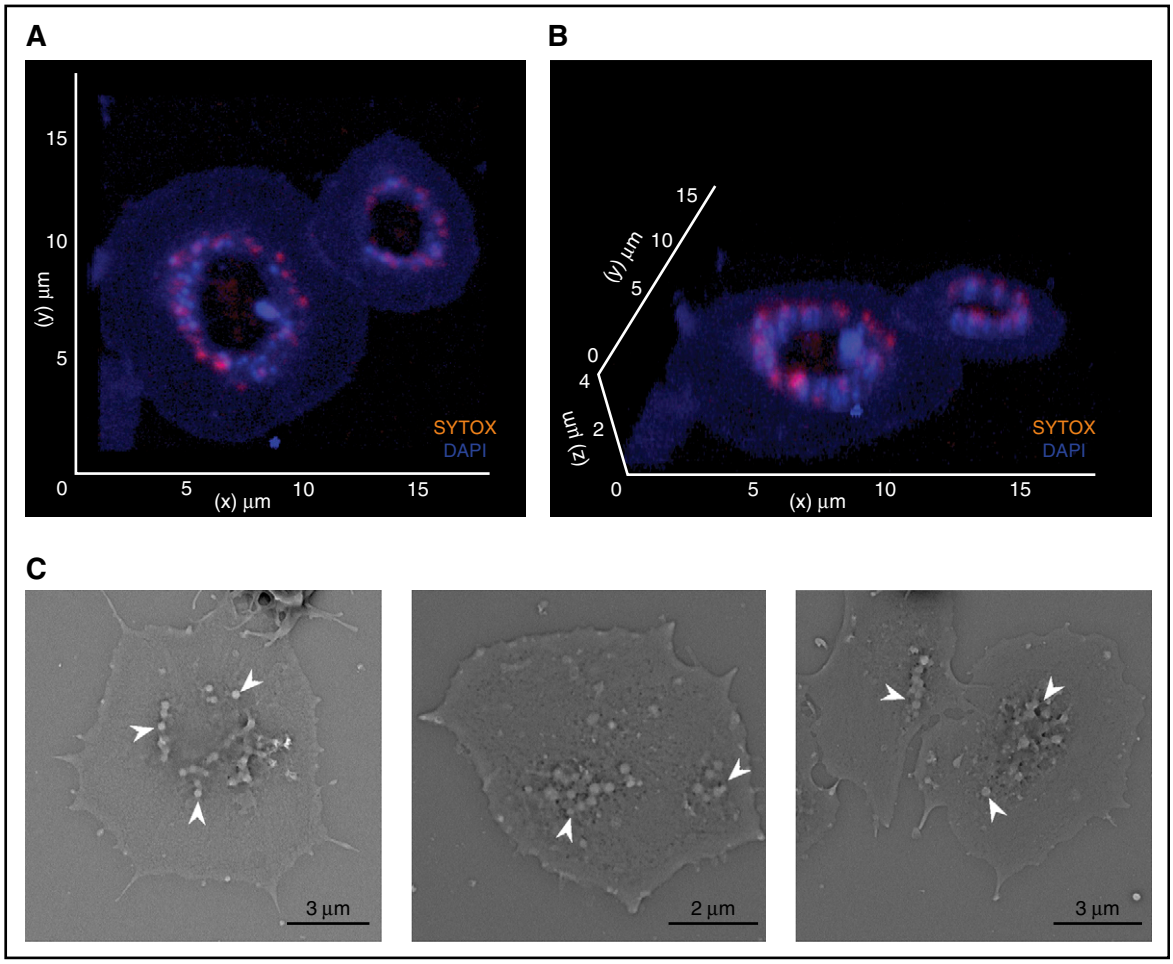

Figure 4. Polyphosphate nanoparticles are retained at the platelet granulomere after release. (A-B) Three-dimensional reconstruction of fixed spread platelets on immobilized VWF, analyzed by confocal microscopy (microscopic images were acquired at a magnification of ×630). Blue, DAPI; orange, SYTOX. (C) Scanning electron microscopy of spreading platelets. Arrows indicate spherical structures.

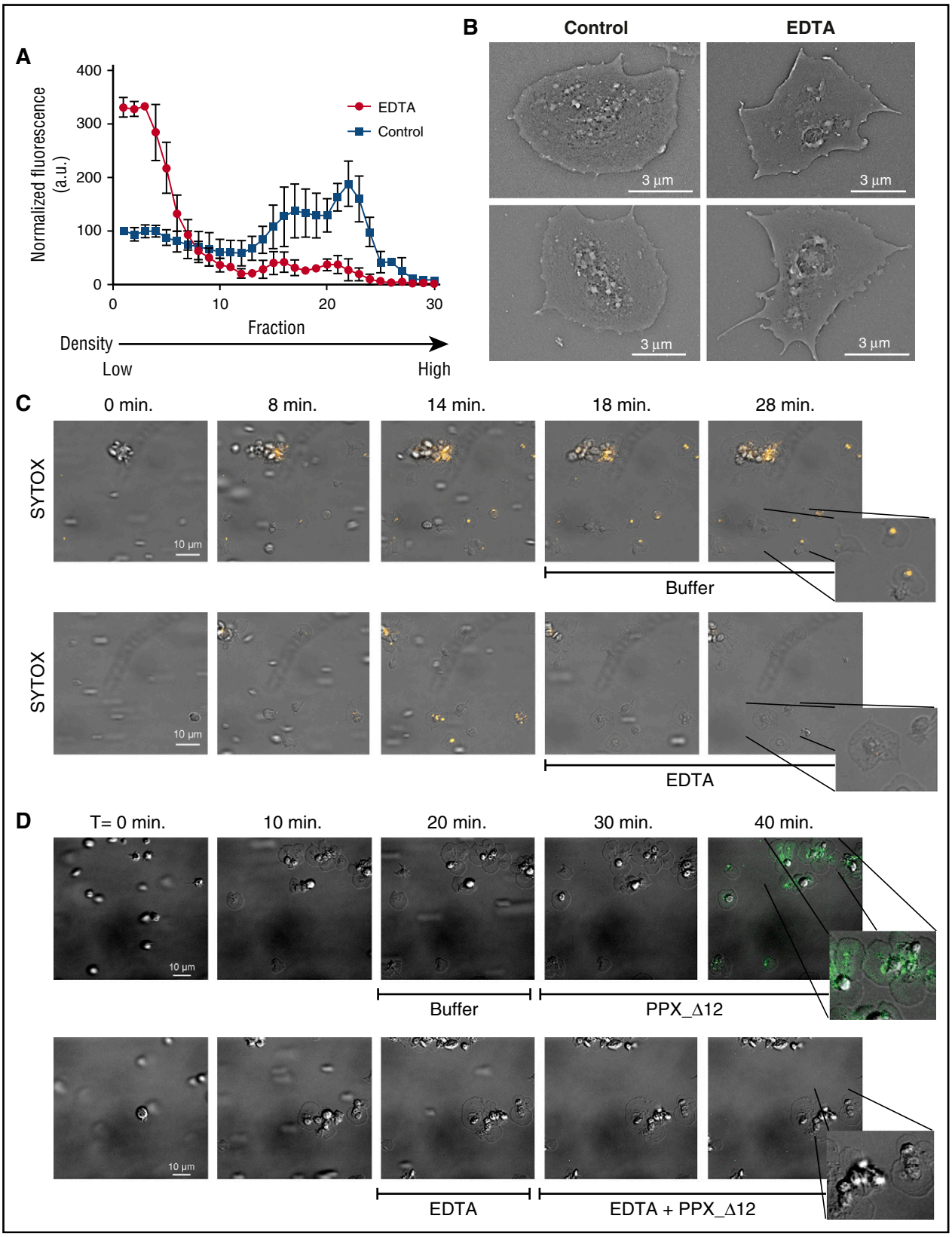

Figure 5. Polyphosphate nanoparticle formation depends on divalent metal ion incorporation and promotes contact system activation. (A) Fractionation of SYTOX-supplemented platelet lysate by ultracentrifugation on sucrose density gradients in the absence or presence of EDTA (250 mM). Data show normalized means ± standard deviation of 3 independent fractionation experiments. (B) Scanning electron microscopy of spreading platelets in the absence or presence of EDTA (250 mM). (C-D) Platelet adhesion and spreading on immobilized VWF under flow. A scale bar is shown in the left panel (10 µm). All images are shown at the same magnification; insets show indicated areas at higher magnification. Times (above) represent the time course, starting from the moment of first stable platelet adhesion in the image field. (C) Polyphosphate exposure was tracked with SYTOX (orange). After 15 minutes, either buffer or EDTA (50 mM) was perfused over spread platelets. (D) Polyphosphate exposure was detected

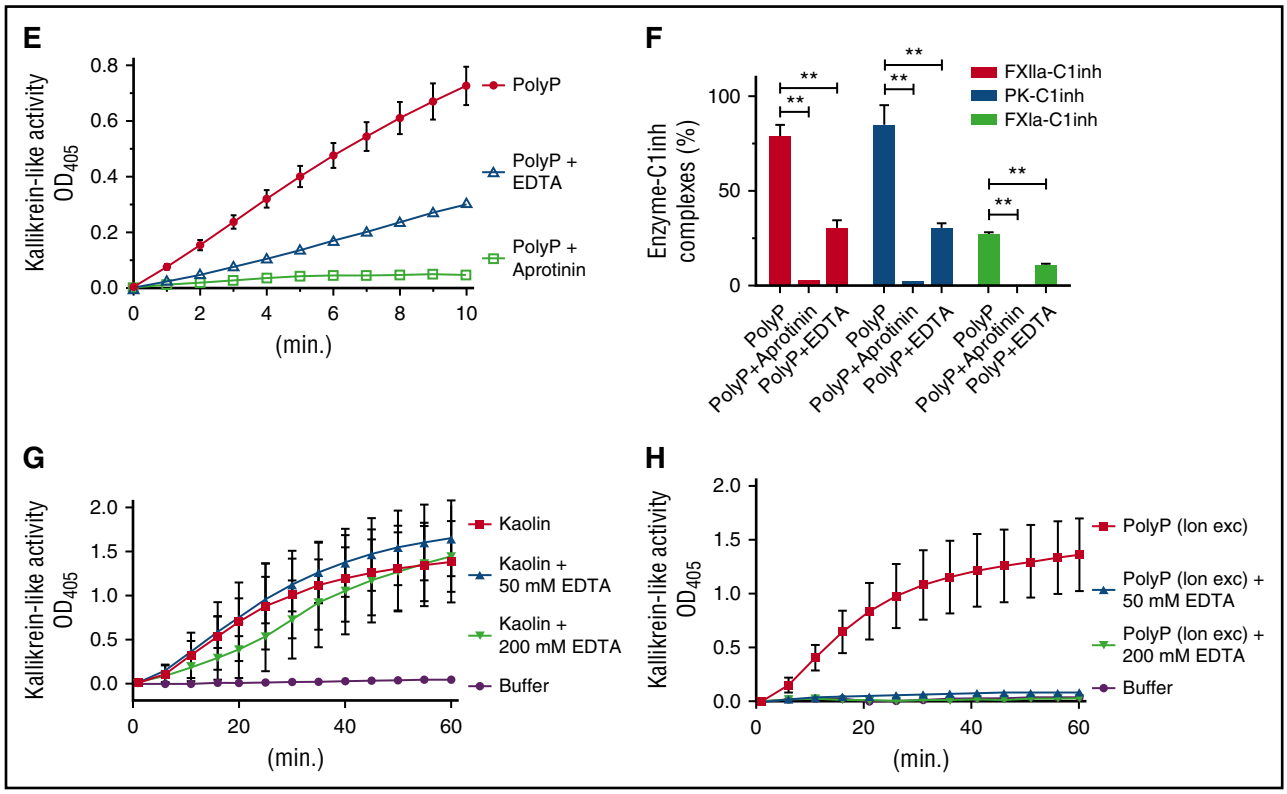

Figure 5. (Continued).

washed platelets over immobilized VWF and tracked polyphosphate mobilization to the cell surface with SYTOX and subsequently exposed platelets to EDTA. As before, polyphosphate mobilization occurred after 4 to 5 minutes (Figure 5C; supplemental Video 5A). Exposure of these cells to EDTA after 15 to 20 minutes of perfusion resulted in immediate removal of polyphosphate from the platelet surface as visualized by SYTOX (Figure 5C; supplemental Video 5B). Similarly, PPX_Δ12 was unable to bind to the platelet surface after exposure to EDTA (Figure 5D; supplemental Video 5C-D).

Polyphosphate nanoparticle formation strongly promotes contact system activation

Finally, we investigated whether platelet polyphosphate nanoparticle formation influenced the ability of polyphosphate to activate the plasma contact system. Hereto, we re-created calcium-polyphosphate nanoparticles with synthetic soluble polyphosphate (70-mers). In a calcium-adsorbed state, this form of polyphosphate was capable of inducing kallikrein-like activity (Figure 5E). It is noteworthy that the apparent polymer size of short polyphosphate increases during calcium complexation, when analyzed in a gel-based assay (supplemental Figure 2). We found that plasma kallikrein-like activity was strongly diminished in the presence of EDTA and completely abrogated by the plasma kallikrein-inhibitor aprotinin, confirming the known importance of plasma kallikrein in contact activation (Figure 5E). We subsequently measured enzyme-C1inh complexes in plasma to investigate activation of the contact system enzymes as well as FXI in more detail. We found that calcium-adsorbed polyphosphate nanoparticles quickly triggered FXIIa-C1inh, PK-C1inh, and FXIa-C1inh complexes (Figure 4F; signals after 15 minutes of incubation; no complexes form in plasma without a trigger; not shown). Aprotinin completely blocked, and EDTA strongly reduced, formation of all these complexes. These findings indicate that the generation of kallikrein-like activity by polyphosphate nanoparticles in plasma is accompanied by activation of FXII, plasma prekallikrein, and FXI.

We then established that contact system activation by kaolin proceeds normally in the presence of EDTA, confirming that contact activation itself could take place without divalent metal ions as a prerequisite (Figure 5G). However, the contact system–activating potential of total platelet polyphosphate (isolated by ion exchange, 20 μM; expressed as monophosphate units) was fully abrogated in the presence of EDTA (Figure 5H). These experiments cumulatively suggest that membrane-associated polyphosphate nanoparticles constitute a powerful trigger for contact system activation.

Figure 5 (continued) by the binding of Alexa488-conjugated PPX_Δ12 (green) after 25 minutes of platelet spreading in the absence or presence of EDTA (250 mM). Microscopic images were acquired at a magnification of ×1000. A scale bar (10 μm) is shown in the first panel of the series. All images are shown at the same magnification. Times (indicated above) represent the time course, starting from the first moment of stable platelet adhesion in the image field. Insets show indicated areas at higher magnification. Images are representative for experiments that were performed >3 times. (E-F) Plasma contact system activation by 50 μg/mL calcium-preadsorbed synthetic short-chain polyphosphate (PolyP; 70-mers). (E) Kallikrein-like activity was monitored by conversion of a chromogenic substrate and (F) formation of enzyme-C1 inhibitor complexes in plasma (after 15 minutes). Where indicated, contact system activation was triggered in the presence of aprotinin (100 U/mL) or by polyphosphate (PolyP) that was pretreated with EDTA (100 mM) for 10 minutes prior to contact system activation. 100% indicates the amount of complexes that are formed in plasma when exposed to positive control contact activators for 30 minutes. $^{**}P < .01$, analyzed by unpaired Student *t* test. (G-H) Kaolin (1.5 μg/mL) or anion exchange–purified platelet polyphosphate (20 μM; expressed as monophosphate units) triggered kallikrein-like activity in the absence or presence of EDTA, monitored by chromogenic substrate conversion.

Discussion

Polyphosphate is an ancient and diverse biological "multi-tool" that regulates a wide variety of biological processes ranging from cell proliferation to angiogenesis, apoptosis, osteoblast function, bone mineralization, energy metabolism, and tumor metastasis.[37] Platelet granules contain large amounts of polyphosphate, and patients with dense-granule defects have ~10 times less polyphosphate in their platelets.[1,38] Moreover, genetic targeting of inositol hexakisphosphate kinase 1 (a key enzyme in polyphosphate biosynthesis) in mice has been shown to reduce platelet polyphosphate content and granule numbers.[39]

Over the past decades, several studies have reported that activated platelets promote coagulation in a FXII-dependent manner.[19-22] More recently, platelet polyphosphate was implicated as the molecular link between platelet activation and FXII activation in vitro[7] and in vivo.[23] These studies analyzed soluble polyphosphate in the supernatant of activated platelets and found that platelets release short-chain polyphosphate polymers. Confusingly, short-chain polyphosphate constitutes a weak activator of FXII.[24,26] At the same time, agents that block polyphosphate polymers have been shown to effectively interfere with platelet-driven thrombus formation without a therapy-associated increased rate of hemorrhage.[12,14] These observations phenocopy the results observed in experimental models of thrombosis performed using either FXII-deficient mice[18] or an antibody that blocks the activation of FXI by FXIIa,[15] suggesting that FXII activation by platelet polyphosphate promotes pathological thrombus formation in vivo. We here identify an additional, previously unidentified pool of platelet polyphosphate, which is retained on the cell surface during and after degranulation. The apparent polymer size of membrane-associated polyphosphate largely exceeds that of secreted soluble polyphosphate polymers. Microscopic analyses as well as ultracentrifugation fractionation studies indicate that membrane-associated platelet polyphosphate adopts a nanoparticle state. The effects of the chelating agent EDTA show that divalent metals are essential for the stability and membrane association of polyphosphate nanoparticles. This observation corresponds well to the biochemical principle that phosphate forms insoluble complexes with divalent metal ions[40] as well as recent reports that synthetic polyphosphate precipitates into stable spherical nanoparticles in the presence of calcium.[29,41] It is attractive to hypothesize that intracellular calcium and other divalent metal ions are stored in a (poly)phosphate-complexed state to avoid the maintenance of steep osmolarity gradients over the phospholipid membrane of intracellular granules. Evidence from microscopy experiments supports this concept: sectioned platelets and isolated dense granules often appear as void lipid bilayers in electron microscopy studies.[1]

FXII requires binding to a surface in order to effectively initiate blood coagulation; example surfaces include silica-based particulates such as glass or kaolin (reviewed in de Maat and Maas[42]). The archetypical FXII activator ellagic acid (a commonly used diagnostic reagent) is a surprising exception. Although this small molecule lacks the properties of a surface, it only triggers FXII activation and subsequent thrombin generation when precipitated into insoluble particles with divalent metal ions.[43] Our findings indicate that the FXII-activating properties of polyphosphate are also controlled by ion-triggered precipitation, complementing the concept that the role of polyphosphate in coagulation is modulated by polymer size.

From previous studies, it has become clear that polyphosphate's polymer size deeply influences its hemostatic functions (as a soluble molecule).[24] Our findings lead to the question of whether polyphosphate will actually meet the bloodstream in a soluble state.

It is often reported that platelets contain short polyphosphate polymers, whereas microorganisms contain much larger polymers. During our studies, we recognized that calcium complexation strongly alters the migratory behavior of polyphosphate, leading to a higher apparent polymer size in gel-based electrophoresis experiments (supplemental Figure 2). In addition, the appearance of platelet membrane–associated polyphosphate in gel-based assays is strikingly similar (Figure 2A-B). These findings indicate that gel-based assays only provide insight into apparent polymer size. However, the actual determination of polymer size requires more a sophisticated approach, such as nuclear magnetic resonance analyses.[23,24]

Recently, polyphosphate was shown to be capable of dampening C1s-mediated activation of the classical pathway by accelerating C1inh neutralization of C1s cleavage of C4 and C2.[6] This study also visualized polyphosphate on activated platelet surfaces, consistent with our findings. Although speculative, it is attractive to hypothesize that polyphosphate nanoparticle formation enables concentration of C1inh on the platelet surface as C1inh colocalizes with polyphosphate.

Mast cells contain crystalline granules that store high levels of concentrated inflammatory mediators as well as heparin. Polyphosphate colocalizes with serotonin and calcium in the acidic secretory granules of mast cells (similar to platelet dense granules) and is released during mast cell activation.[2] In separate reports, mast cells were shown to secrete stable, solid particles that can deliver signals to remote lymph nodes.[44] Based on these combined observations, it is attractive to speculate that mast cells also contain solid polyphosphate nanoparticles. This hypothesis would provide a mechanistic explanation for the increased activity of the coagulation system[45] and activation of the plasma contact system[46,47] observed in mast cell–related disorders.

In conclusion, our findings may provide a new perspective on the procoagulant role of platelet polyphosphate as well as refine our view on the mechanisms by which platelets distribute their granular content.

Acknowledgments

The authors gratefully acknowledge the expertise and assistance of the Cell Microscopy Center Utrecht.

The authors gratefully acknowledge financial support (C.M.) of the International Patient Organization for C1-Inhibitor Deficiencies, Stichting Vrienden van Het UMC Utrecht, and The Netherlands Organization for Scientific Research. T.R. was supported by the Hjärt Lungfonden (20140741), Stockholms Läns Landsting (ALF; 20140464), Vetenskapsrådet (K2013-65X-21462-04-5), the German Research Society (SFB877, TP A11 and SFB841, TP B8), and a European Research Council grant (ERC-StG-2012-311575_F-12). O.J.T.M. was supported by grants from the National Institutes of Health (National Heart, Lung, and Blood Institute, R01 HL101972, and National Institute of General Medical Sciences, R01 GM116184) and the American Heart Association (13EIA12630000).

Authorship

Contribution: J.J.F.V., A.D.B., K.F.N., K.D., S.d.M., E.K., L.L., A.P.H., and M.H.F. performed experiments; T.R., S.d.M., and

C.M. designed the experiments; H.F.H., R.S., and H.S. provided critical reagents and expertise; J.J.F.V., A.D.B., K.F.N., T.R., O.J.T.M., and C.M. drafted and edited the manuscript; and all authors approved the final manuscript.

Conflict-of-interest disclosure: The authors declare no competing financial interests.

ORCID profiles: J.J.F.V., 0000-0003-2483-597X; A.D.B., 0000-0002-0653-5538; K.F.N., 0000-0003-1287-6766; E.K., 0000-0002-2784-5244; L.L., 0000-0002-1858-867X; O.J.T.M., 0000-0001-9481-0124; R.S., 0000-0002-1012-9815; H.F.H., 0000-0002-8819-9231; M.H.F., 0000-0002-0515-8806; S.d.M., 0000-0003-1179-374X; T.R., 0000-0003-4594-5975; C.M., 0000-0003-4593-0976.

Correspondence: Coen Maas, Department of Clinical Chemistry and Haematology, University Medical Center Utrecht, Heidelberglaan 100, Room G.03.550, 3584CX Utrecht, The Netherlands; e-mail: cmaas4@umcutrecht.nl.

References

1. Ruiz FA, Lea CR, Oldfield E, Docampo R. Human platelet dense granules contain polyphosphate and are similar to acidocalcisomes of bacteria and unicellular eukaryotes. *J Biol Chem*. 2004; 279(43):44250-44257.
2. Moreno-Sanchez D, Hernandez-Ruiz L, Ruiz FA, Docampo R. Polyphosphate is a novel pro-inflammatory regulator of mast cells and is located in acidocalcisomes. *J Biol Chem*. 2012;287(34): 28435-28444.
3. Nickel KF, Ronquist G, Langer F, et al. The polyphosphate-factor XII pathway drives coagulation in prostate cancer-associated thrombosis. *Blood*. 2015;126(11):1379-1389.
4. Montilla M, Hernández-Ruiz L, García-Cozar FJ, Alvarez-Laderas I, Rodríguez-Martorell J, Ruiz FA. Polyphosphate binds to human von Willebrand factor in vivo and modulates its interaction with glycoprotein Ib. *J Thromb Haemost*. 2012;10(11): 2315-2323.
5. Brandt S, Krauel K, Jaax M, et al. Polyphosphates form antigenic complexes with platelet factor 4 (PF4) and enhance PF4-binding to bacteria. *Thromb Haemost*. 2015;114(6):1189-1198.
6. Wijeyewickrema LC, Lameignere E, Hor L, et al. Polyphosphate is a novel cofactor for regulation of complement by a serpin, C1 inhibitor. *Blood*. 2016;128(13):1766-1776.
7. Smith SA, Mutch NJ, Baskar D, Rohloff P, Docampo R, Morrissey JH. Polyphosphate modulates blood coagulation and fibrinolysis. *Proc Natl Acad Sci USA*. 2006;103(4):903-908.
8. Choi SH, Smith SA, Morrissey JH. Polyphosphate is a cofactor for the activation of factor XI by thrombin. *Blood*. 2011;118(26):6963-6970.
9. Choi SH, Smith SA, Morrissey JH. Polyphosphate accelerates factor V activation by factor XIa. *Thromb Haemost*. 2015;113(3):599-604.
10. Puy C, Tucker EI, Ivanov IS, et al. Platelet-derived short-chain polyphosphates enhance the inactivation of tissue factor pathway inhibitor by activated coagulation factor XI. *PLoS One*. 2016; 11(10):e0165172.
11. Mutch NJ, Engel R, Uitte de Willige S, Philippou H, Ariëns RAS. Polyphosphate modifies the fibrin network and down-regulates fibrinolysis by attenuating binding of tPA and plasminogen to fibrin. *Blood*. 2010;115(19):3980-3988.
12. Travers RJ, Shenoi RA, Kalathottukaren MT, Kizhakkedathu JN, Morrissey JH. Nontoxic polyphosphate inhibitors reduce thrombosis while sparing hemostasis. *Blood*. 2014;124(22): 3183-3190.
13. Zhu S, Travers RJ, Morrissey JH, Diamond SL. FXIa and platelet polyphosphate as therapeutic targets during human blood clotting on collagen/tissue factor surfaces under flow. *Blood*. 2015; 126(12):1494-1502.
14. Labberton L, Kenne E, Long AT, et al. Neutralizing blood-borne polyphosphate in vivo provides safe thromboprotection. *Nat Commun*. 2016;7:12616.
15. Matafonov A, Leung PY, Gailani AE, et al. Factor XII inhibition reduces thrombus formation in a primate thrombosis model. *Blood*. 2014;123(11):1739-1746.
16. Revenko AS, Gao D, Crosby JR, et al. Selective depletion of plasma prekallikrein or coagulation factor XII inhibits thrombosis in mice without increased risk of bleeding. *Blood*. 2011;118(19): 5302-5311.
17. Yau JW, Liao P, Fredenburgh JC, et al. Selective depletion of factor XI or factor XII with antisense oligonucleotides attenuates catheter thrombosis in rabbits. *Blood*. 2014;123(13):2102-2107.
18. Renné T, Pozgajová M, Grüner S, et al. Defective thrombus formation in mice lacking coagulation factor XII. *J Exp Med*. 2005;202(2):271-281.
19. Castaldi PA, Larrieu MJ, Caen J. Availability of platelet Factor 3 and activation of factor XII in thrombasthenia. *Nature*. 1965;207(995):422-424.
20. Walsh PN, Griffin JH. Platelet-coagulant protein interactions in contact activation. *Ann N Y Acad Sci*. 1981;370:241-252.
21. Johne J, Blume C, Benz PM, et al. Platelets promote coagulation factor XII-mediated proteolytic cascade systems in plasma. *Biol Chem*. 2006;387(2):173-178.
22. Bäck J, Sanchez J, Elgue G, Ekdahl KN, Nilsson B. Activated human platelets induce factor XIIa-mediated contact activation. *Biochem Biophys Res Commun*. 2010;391(1):11-17.
23. Müller F, Mutch NJ, Schenk WA, et al. Platelet polyphosphates are proinflammatory and procoagulant mediators in vivo. *Cell*. 2009;139(6): 1143-1156.
24. Smith SA, Choi SH, Davis-Harrison R, et al. Polyphosphate exerts differential effects on blood clotting, depending on polymer size [published correction appears in *Blood*. 2011;117(12):3477]. *Blood*. 2010;116(20):4353-4359.
25. Morrissey JH, Smith SA. Polyphosphate as modulator of hemostasis, thrombosis, and inflammation. *J Thromb Haemost*. 2015;13(Suppl 1): S92-S97.
26. Puy C, Tucker EI, Wong ZC, et al. Factor XII promotes blood coagulation independent of factor XI in the presence of long-chain polyphosphates. *J Thromb Haemost*. 2013;11(7):1341-1352.
27. Holmsen H, Weiss HJ. Secretable storage pools in platelets. *Annu Rev Med*. 1979;30:119-134.
28. Fitch-Tewfik JL, Flaumenhaft R. Platelet granule exocytosis: a comparison with chromaffin cells. *Front Endocrinol (Lausanne)*. 2013;4:77.
29. Donovan AJ, Kalkowski J, Smith SA, Morrissey JH, Liu Y. Size-controlled synthesis of granular polyphosphate nanoparticles at physiologic salt concentrations for blood clotting. *Biomacromolecules*. 2014;15(11):3976-3984.
30. Remijn JA, Wu YP, Ijsseldijk MJ, Zwaginga JJ, Sixma JJ, de Groot PG. Absence of fibrinogen in afibrinogenemia results in large but loosely packed thrombi under flow conditions. *Thromb Haemost*. 2001;85(4):736-742.
31. Rouser G, Fkeischer S, Yamamoto A. Two dimensional then layer chromatographic separation of polar lipids and determination of phospholipids by phosphorus analysis of spots. *Lipids*. 1970;5(5):494-496.
32. Summer H, Grämer R, Dröge P. Denaturing urea polyacrylamide gel electrophoresis (Urea PAGE). *J. Vis. Exp. JoVE*. 2009;(32):
33. Smith SA, Morrissey JH. Sensitive fluorescence detection of polyphosphate in polyacrylamide gels using 4′,6-diamidino-2-phenylindol. *Electrophoresis*. 2007;28(19):3461-3465.
34. de Maat S, Björkqvist J, Suffritti C, et al. Plasmin is a natural trigger for bradykinin production in patients with hereditary angioedema with factor XII mutations. *J Allergy Clin Immunol*. 2016;138(5): 1414-1423.e9.
35. Nishibori M, Cham B, McNicol A, Shalev A, Jain N, Gerrard JM. The protein CD63 is in platelet dense granules, is deficient in a patient with Hermansky-Pudlak syndrome, and appears identical to granulophysin. *J Clin Invest*. 1993; 91(4):1775-1782.
36. Fuchs TA, Brill A, Duerschmied D, et al. Extracellular DNA traps promote thrombosis. *Proc Natl Acad Sci USA*. 2010;107(36):15880-15885.
37. Morrissey JH, Choi SH, Smith SA. Polyphosphate: an ancient molecule that links platelets, coagulation, and inflammation. *Blood*. 2012;119(25):5972-5979.
38. Hernández-Ruiz L, Sáez-Benito A, Pujol-Moix N, Rodríguez-Martorell J, Ruiz FA. Platelet inorganic polyphosphate decreases in patients with delta storage pool disease. *J Thromb Haemost*. 2009; 7(2):361-363.
39. Ghosh S, Shukla D, Suman K, et al. Inositol hexakisphosphate kinase 1 maintains hemostasis in mice by regulating platelet polyphosphate levels. *Blood*. 2013;122(8):1478-1486.
40. Binas English Edition. Handbook for Physics, Chemistry, Biology and Mathematics. Groningen, The Netherlands: Wolters-Noordhoff; 2007.
41. Donovan AJ, Kalkowski J, Szymusiak M, et al. Artificial dense granules: a procoagulant liposomal formulation modeled after platelet polyphosphate storage pools. *Biomacromolecules*. 2016;17(8):2572-2581.
42. de Maat S, Maas C. Factor XII: form determines function. *J Thromb Haemost*. 2016;14(8):1498-1506.
43. Bock PE, Srinivasan KR, Shore JD. Activation of intrinsic blood coagulation by ellagic acid: insoluble ellagic acid-metal ion complexes are the activating species. *Biochemistry*. 1981;20(25):7258-7266.
44. Kunder CA, St John AL, Li G, et al. Mast cell-derived particles deliver peripheral signals to remote lymph nodes. *J Exp Med*. 2009;206(11): 2455-2467.
45. Cugno M, Marzano AV, Asero R, Tedeschi A. Activation of blood coagulation in chronic urticaria: pathophysiological and clinical implications. *Intern Emerg Med*. 2010;5(2):97-101.
46. Sala-Cunill A, Björkqvist J, Senter R, et al. Plasma contact system activation drives anaphylaxis in severe mast cell-mediated allergic reactions. *J Allergy Clin Immunol*. 2015;135(4):1031-43.e6.
47. Oschatz C, Maas C, Lecher B, et al. Mast cells increase vascular permeability by heparin-initiated bradykinin formation in vivo. *Immunity*. 2011; 34(2):258-268.

2017 129: 1707-1717
doi:10.1182/blood-2016-08-734988 originally published online January 3, 2017

Polyphosphate nanoparticles on the platelet surface trigger contact system activation

Johan J. F. Verhoef, Arjan D. Barendrecht, Katrin F. Nickel, Kim Dijkxhoorn, Ellinor Kenne, Linda Labberton, Owen J. T. McCarty, Raymond Schiffelers, Harry F. Heijnen, Antoni P. Hendrickx, Huub Schellekens, Marcel H. Fens, Steven de Maat, Thomas Renné and Coen Maas

Blood (print ISSN 0006-4971, online ISSN 1528-0020), is published weekly by the American Society of Hematology, 2021 L St, NW, Suite 900, Washington DC 20036.